NUKLEONIKA 2022;67(3):49–64
doi: 10.2478/nuka-2022-0005

TECHNICAL REPORT

sciendo

Recent upgrading of the nanosecond pulse radiolysis setup and construction of laser flash photolysis setup at the Institute of Nuclear Chemistry and Technology in Warsaw, Poland

Tomasz Szreder

Abstract. Modification of pulse radiolysis (PR) setup and construction of a new laser flash photolysis (LFP) setup at the Institute of Nuclear Chemistry and Technology (INCT) is described. Both techniques are dedicated to studying fast reactions in real time by direct observation of transients. Time resolution of the PR setup at INCT was ~11 ns, limited by the duration of the electron pulse. Implementation of a new spectrophotometric detection system resulted in a significant broadening of experimental spectral range with respect to the previous setup. Noticeable reduction of the noise-to-signal ratio was also achieved. The LFP system was built from scratch. Its time resolution was ~6 ns, limited by the duration of a laser pulse. LFP and PR were purposely designed to share the same hardware and software solutions. Therefore, components of the detection systems can be transferred between both setups, significantly lowering the costs and shortening the construction/upgrading time. Opened architecture and improved experimental flexibility of both techniques were accomplished by implementation of Ethernet transmission control protocol/Internet protocol (TCP/IP) communication core and newly designed software. This is one of the most important enhancements. As a result, new experimental modes are available for both techniques, improving the quality and reducing the time of data collections. In addition, both systems are characterized by relatively high redundancy. Currently, implementation of new equipment into the systems hardly ever requires programming. In contrast to the previous setup, daily adaptations of hardware to experimental requirements are possible and relatively easy to perform.

Keywords: Computer-controlled systems • Data collection software • Data processing software • Laser flash photolysis • Pulse radiolysis • Time-resolved techniques

Introduction

Pulse radiolysis (PR) and laser flash photolysis (LFP) are time-resolved techniques developed for studies of fast chemical reactions and physical processes. The operating principles of both techniques inherited the idea from flash photolysis. The first flash photolysis system with millisecond time resolution was introduced to scientists by Norrish and Porter in 1949 [1] and Porter in 1950 [2]. They jointly won the Nobel Prize in Chemistry in 1967 for this invention [3]. The PR technique was introduced in 1960 simultaneously by several independent researchers form different scientific centers [4–8]. The first investigations applying LFP systems were published several years later [9, 10]. Within years, these techniques became more powerful and sophisticated due to the developments in electronics and optics. Currently, even attosecond-level time resolution systems are available [11]. Interest in these methods grew considerably as the practical applications expanded from chemistry to biology, materials science, environmental sciences, etc. It is

T. Szreder
Institute of Nuclear Chemistry and Technology
Dorodna 16 Str., 03-195 Warszawa, Poland
E-mail: t.szreder@ichtj.waw.pl

Received: 28 July 2022
Accepted: 16 August 2022

important to note that both the techniques, i.e., LFP and PR, are considered complementary techniques. This has been demonstrated many times in literature [12]. Complete explanation of the observed changes in the investigated systems very often requires combined results from both techniques. Therefore, it is very convenient to have LFP and PR available at one laboratory.

LFP systems are quite common in scientific laboratories, whereas PR facilities are rather limited. For instance, two PR systems are available in Poland: the first one, at the Institute of Nuclear Chemistry and Technology in Warsaw (INCT) [13]; and the second, at the Institute of Applied Chemistry and Technology in Lodz [14]. Both systems work with nanosecond time resolution. In Europe, one more picosecond PR facility is available in France [15]. Several other similar facilities are available in China, India, Japan, and the USA.

Both LFP and PR may operate with various detections systems, such as ultraviolet–visible–near infrared (UV–VIS–NIR) or infrared (IR) spectrophotometry, Raman spectroscopy, conductometry, electron paramagnetic resonance (EPR), nuclear magnetic resonance (NMR), light scattering (LS), etc. [14, 16, 17]. Moreover, they can use transient digitizer or pump(pulse)–probe data collection systems [15]. At the INCT, both LFP and PR operate with transient digitizer UV–VIS–NIR spectrophotometric detection. The operational principles of this technique are depicted in Fig. 1. A beam of analytical light that continuously passes through the sample is split on a monochromator or passes through a narrow bandpass filter. The intensity of a selected wavelength of light is monitored by a fast photodetector. The signal intensity remains constant until the delivery of a high-energy pulse (from a pulse source), initiating photolysis/radiolysis of the sample. The energy of the pulse absorbed in a sample causes the formation of transients and/or stable products. This affects the spectral characteristics of the system studied, which is reflected by a change in the detector photocurrent. Digitized and processed detector responses are used for kinetic analysis and identification of the reacting species by their spectroscopic footprints, eventually. Lasers in LFP and electron accelerators in PR are usually used as the sources of high-energy pulses.

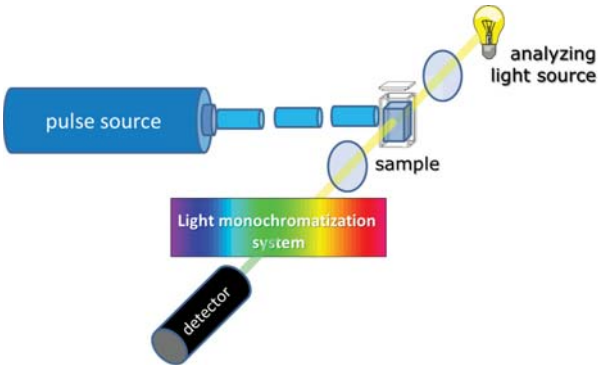

Fig. 1. Simplified diagram illustrating the operation principle of laser flash photolysis and pulse radiolysis with fast spectrophotometric detection.

The construction concept of the LAE-10 pulse electron accelerator dedicated solely to PR at the INCT dates back to the 90s of the 20th century [18]. Regular experiments were started at the beginning of the millennium [13, 19]. The early design of the PR at the INCT was oriented toward the spectroscopic study of fast chemical processes involving radicals in biological or related systems at room temperature. In most of the cases, it required the same experimental setup and methodology. Therefore, the first-designed PR system coupled with LAE-10 linear accelerator was oriented toward a relatively closed hardware and software architecture [13]. Such a concept caused certain limitations in experimental flexibility. Over time, studies of other systems (e.g., spent nuclear fuel reprocessing systems [20], supramolecular systems [21], ionic liquid systems [22], waste decomposition [23], etc.) became equally important. Apart from that, the old worn parts of the PR system required replacement. Therefore, adaptations of new hardware components, data acquisition, and data processing techniques have become necessary in order to comply with current research requirements. Significant progress in the fields of computer technology, electronics, optoelectronics, and optics made such upgrading quite difficult due to incompatibility of the new and old technological solutions. Moreover, the closed architecture of the older system was an additional obstacle.

Upgrading of the PR system started from its simplification by the elimination of redundant (not used anymore) components and the replacement of unconventional, homemade electronic and optoelectrical components by standard and commercially available products. Our efforts were focused on building a relatively simple, user-friendly experimental environment with an opened architecture available for easy adaptation of new subsystems (flexibility). Additional concept premises relied on reduction of the recorded noise-to-signal ratio and the design of automatic, fast, and human-error-resistant control/data acquisition software. Unification and extension of hardware communication between detection and accelerator control subsystems with full LAE-10 computer control is planned in the next step. Description of a new system has never been published before. A previous publication [24] depicted the state of PR at the INCT before 2009 and, in some points, is misleading (particularly, description of the detection system). It is worth mentioning that the introduced communication core and closely interacting software, in a new version of PR, is unique for this kind of instruments. It provides enormous flexibility and a wide range of possibilities for this technique.

Simultaneously, the LFP system with nanosecond time resolution at the INCT was built from scratch. As far as it was possible, the LFP uses the same hardware and software solutions as at the PR system. This significantly lowers the development/maintaining costs and shortens the construction time. Moreover, the application of the same data acquisition and data processing software for both techniques is very convenient for regular users. This is particularly prominent in studies requiring the involvement of both techniques.

Pulse radiolysis system

Source of electron pulse – the LAE-10 accelerator

The LAE-10 is a linear electron accelerator designed and manufactured at the INCT. Its structure is partially based on components purchased in the former Soviet Union. Electron acceleration is achieved in the LAE-10 by a gradient of the electric field of an electromagnetic wave component using the so-called travelling wave mechanism. The electromagnetic field is generated by a high-frequency system based on two klystrons: KIU 17 (pulse power: 100 kW) and KIU 15 (pulse power: 20 MW). The system operates with a frequency of ~1818 MHz. A triode--type electron gun with a porous tungsten cathode is used as a source of electrons. The resulting electron energies of the LAE-10 are ~10 MeV with a maximum pulse beam current of 1 A. More details on the construction of the LAE-10 accelerator can be found in previous publications [18, 24]. In regular daily experiments, the LAE-10 operates with a short ~11-ns single-pulse mode (however, repetitions up to 5 Hz and 100-ns pulses are also available). The typical pulse characteristics recorded by three different methods are shown in Fig. 2. Time durations measured as the full width at half maximum (FWHM) are ~10–12 ns. It is important to notice that a main pulse is followed by a smaller signal. This signal can be significantly reduced by increasing the reverse voltage on the electron gun grid. However, this operation also decreases the dose delivered by the electron pulse.

The dose delivered by an electron pulse is measured by a Faraday cup placed after the sample cell holder in the axis of the electron beam. The signal from a Faraday cup is recorded and processed (area integration) using a WaveRunner 6051A LeCroy digital oscilloscope (8-bit vertical resolution, 5 GS/s sample rate, 500 MHz bandwidth). The highest doses delivered by 10-ns pulses are ~20 Gy.

The electrical signal triggered by the electron gun is processed and sent by fiber optics to the detection system. The jitter measured between the Cherenkov radiation and the triggering signal of the detection system is ~2.5 ns.

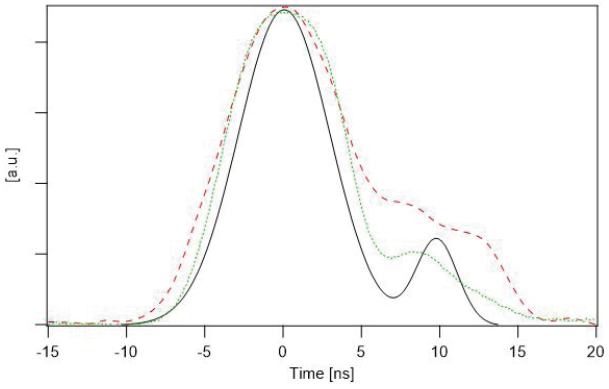

Fig. 2. Pulse time duration recorded as the first derivative of a signal recorded at 700 nm for pulse-irradiated Ar-saturated water (solid black line); the Faraday cup signal (dashed red line), and the Cherenkov radiation recorded for pulse-irradiated Ar-saturated water at 390 nm (dotted green line).

Detection system

There are two available analyzing light sources at the detection system of PR at the INCT. The first one is the Hamamatsu Photonics K.K. light source, consisting of a quiet (low-noise) L2273 xenon lamp (150 W) placed in E7536 housing and powered by C8849 supply. Alternatively, the currently installed, Newport Corporation system, is based on 6269 UV-enhanced, 1-kW xenon lamp located in 66921 housing and powered by OPS-A1000 (Oriel Instruments). The latter light source is fully computer-controlled via RS-232 interface. The housings of both light sources are equipped with internal reflecting rare mirrors and output lenses to provide a high intensity of the relatively collimated analyzing light beams. The arc axes of both systems are perpendicular to the axis of the optical pathway. This eliminates the blind central spot observed in coaxial systems. The potential spectral range for both systems starts at least at 200 nm and ends at wavelengths >2000 nm. The diameter of the output beam of the Hamamatsu Photonics K.K. system is slightly <30 mm, whereas for the Newport Corporation system, it is 48 mm. Basically, the Newport Corporation system provides more-intensive light. Thus, it facilitates collection of experimental data in deep-UV or deep-NIR wavelengths and provides a lower noise-to-signal ratio. However, for light--sensitive samples, the Hamamatsu Photonics K.K. system is recommended. There is no lamp-pulsing system in our setup. This significantly simplifies the hardware-triggering time sequence and allows us to expand the time scales of observation up to seconds.

The optical pathway is adapted to the available light sources in order to maximize the intensity of the light reaching the detectors. It is depicted in Fig. 3. An F150 planoconvex lens (focal length 150 mm, UV-fused silica; Thorlabs Inc.) is used for focusing the analyzing light on the irradiated sample (S). After passing through the sample, beam collimation is restored by a second F150 lens. Practical tests show that the location of an F75 lens (focal length 75 mm, UV-fused silica; Thorlabs Inc.) between the sample and the second F150 lens minimizes losses of light intensity. Finally, the analyzing light beam is redirected almost perpendicularly by an Al-covered

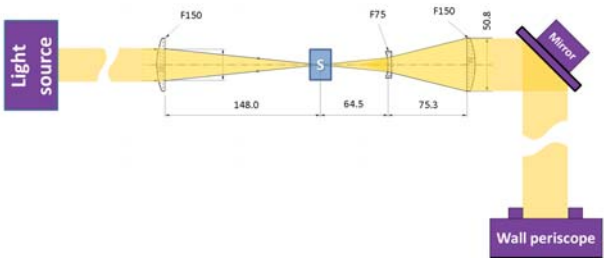

Fig. 3. Simplified scheme of the optical pathway of the PR system in the irradiation chamber (PR IC). S – sample; F150, F75 – lenses.

planar mirror (M) to the two-mirror periscope system placed in a radiation chamber wall (which is a part of the originally built system). The periscope directs the analyzing light to the PR control room (PR CR) where the detection systems are installed.

Exposition of the irradiated sample to the monitoring light is controlled by a mechanical shutter. The shutter is located between the light source and the first F150 lens. We use a homemade shutter, which is based on a central locking actuator for cars. This shutter is capable of performing an open/close cycle within a 1-s time frame. The status of the shutter is monitored by microswitches built into the actuator. The shutter is equipped with an active cooling system to withstand the extensive heat deposition by the 1-kW light source. Moreover, it is fully computer-controlled by an input/output (I/O) ADAM module (Advantech).

A water filter (optical length 10 cm) is used to remove (if it is required) the IR spectral range from the analyzing light spectra. This filter is located between the shutter and the first F150 lens. In order to avoid the effects of photodecomposition and/or photobleaching of samples, UV or VIS cutoff filters are used. They are automatically changed by an RS-232 controlled 10MWA168 – motorized variable wheel (Standa) located between the first F150 lens and the sample (S, Fig. 3).

At the PR control room (PR CR), an analytical light is focused by the UV-fused silica lens (focal length 250 mm, diameter 110 mm) on a monochromator slit or alternatively redirected by an Al-covered planar mirror to a bandpass filter automatic wheel. The required position of the mirror is currently set manually, but in the future, an automatic system will be installed. The monochromatic light for the photomultiplier (PMT) and intensified charge-coupled device (ICCD) detectors is generated by an MSH-301 monochromator (Lot Oriel Gruppe). It is an f/3.9 motorized monochromator/spectrograph with in-plane Czerny–Turner type of optics with a focal length of 260 mm. It supports three, individually replaceable gratings. Their current setup is listed in Table 1.

The MSH-301 monochromator/spectrograph has two optical output ports used for the PMT and ICCD detectors. The desired port is selected by the position of the built-in mirror. Grating 1 (Table 1) is exclusively dedicated for the ICCD detector, whereas gratings 2 and 3 are for the PMT detector. The

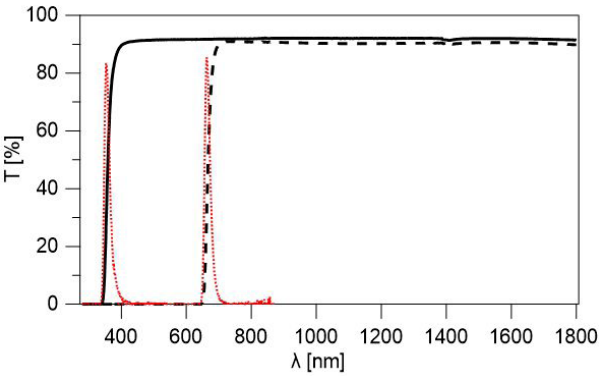

Fig. 4. Optical characteristics of the cutoff filters BK-7 (solid line) and RG-5 (dash line) used in the automatic filter wheel in front of the MSH-301 monochromator. The dotted lines represent the first derivative of the transmittance *T*.

MSH-301 integrated fast electronic shutter is very useful for protection of detectors from long exposition to intensive monitoring light, particularly when used with software oriented on hardware protection. An automatic-cutoff (colored) filter-wheel changer MSZ-121 (Lot Oriel Gruppe) is used in front of the MSH-301. The spectral properties of the two installed cutoff filters BK-7 and RG-5 are shown in Fig. 4. These filters are crucial to prevent transmission of the second harmonic wavelength by the gratings. Experimentally verified, recommended wavelengths for application with BK-7 and RG-5 filters are >415 nm and >685 nm, respectively. The MSH-301 is a fully automated device controlled through an RS232 interface.

An automatic entrance slit based on the Z625B motorized actuator (Thorlabs) is installed in front of the MSH-301. It is particularly important for control of the light intensity reaching the ICCD detector. In general, the spectral resolutions in our experiments are ±7.5 nm and ±15 nm for the PMT and ICCD detectors, respectively. These values correspond to 1 mm of entrance and output (if applicable) slit/s.

The R955 (Hamamatsu) PMT is the most commonly used detector in our system (Table 2). The PMT is attached to the axial port of MSH-301 and placed in a homemade metal housing. The housing protects the PMT from both external electromagnetic noise and external, undesirable light. The R955 spectral response is in the range of 160–900 nm. However, the experimentally available range is nar-

Table 1. Description of available gratings of the MSH-301 monochromator/spectrograph

ID	Spectral range (nm)	Blaze (nm)	Lines (g/mm)	Resolution per slit size (nm/mm)	Comment
1	260–900	500	300	30	Intended for use with the ICCD detector; cutoff filters are required depending on the measurement range
2	250–525	350	1200	15	Dedicated for the PMT detector; recommended for wavelengths <525 nm; a BK-7 cutoff filter is required for wavelengths >415 nm
3	520–1200	750	1200	15	Dedicated for the PMT detector; recommended for wavelengths >525 nm; RG-5 filter is required for wavelengths >685 nm

Table 2. List of available detectors at the INCT PR system

Model (Manufacturer)	Spectral range (nm)	Rise time/time resolution (ns)	Comment
R955 (Hamamatsu)	160–900[1]	Subnanoseconds[4]	PMT detector
iSTAR A-DH720-18F-03 (Andor)	180–850[2]	<5	ICCD detector
PDA10A (Thorlabs)	200–1100[3]	2.3	Silicon-amplified photodiode
APD430A2/M (Thorlabs)	200–1000[3]	<0.88	UV-enhanced, silicon avalanche photodiode
PDA10CF (Thorlabs)	800–1700	2.3	InGaAs-amplified photodiode

[1] Spectral range narrows to 250–760 nm under experimental conditions.
[2] Spectral range narrows to 300–700 nm under experimental conditions.
[3] Noise-to-signal ratio measured by the photodiode is advantageous at wavelengths >520 nm with respect to the PMT detector.
[4] Rise time of the detector with a standard voltage divider is 2.2 ns.

rowed to wavelengths between 250 nm and 760 nm. The maximum sensitivity of the PMT is at ~400 nm. A typical anode time response is 2.2 ns. However, application of a nonstandard voltage divider in our setup improves the time response to subnanosecond time resolution. The design of the voltage divider is based on Beck's [25] description. Only four out of nine dynodes are gradually polarized by a high voltage. Shorted fifth and sixth dynodes provide the output signal. This solution has some limitation. A linear response of the detector is obtained only for a supply voltage <1000 V and an output current <0.8 mA. The PMT detector is powered by a PS310 (Stanford Research Systems) high-voltage supply. This is a general purpose interface bus (GPIB)--controlled device.

In general, we do not use any amplification of the output signal from the PMT. However, some promising tests have been performed using an OPA2694 (Texas Instruments) dual, low-power, 670-MHz-bandwidth operational amplifier. Each of the two OPA2694 integrated circuit blocks is capable of amplifying the signal by a factor of ~8, with a positive or negative polarization. Therefore, it is possible to obtain a 16-fold amplification in total by adding the digitized signals from both the OPA2694 blocks on separate oscilloscope channels. The signals recorded on a single oscilloscope channel do not exceed ±0.5 V, which is a limit of the vertical offset of numerous commercially available digitizers (including the one used in our system). In addition, the advantage of this solution is the possibility of the elimination of noise picked up by cables. By application of the OPA2694, there was an experimentally tested, total reduction of the noise-to-signal ratio at least by a factor of two.

The iSTAR A-DH720-18F-03 (Andor) ICCD detector (Table 2) is attached to the lateral port of the MSH-301. This detector is equipped with a W-type photocathode, an 18-mm-diameter multichannel plate (MCP) image intensifier, and a 1024 × 256 pixel CCD (active pixels: 690 × 256). The size of the CCD pixels is 26 × 26 μm. The minimum gate time of this detector is <5 ns. The spectral range of the iSTAR A-DH720-18F-03 is 180–850 nm, but only 300–700 nm is experimentally available in our setup. In particular cases, the ICCD camera has a great advantage over PMT data collection. It allows the collection of spectrum using small, submilliliter volumes of valuable samples (e.g., DNA [26]). The ICCD trigger pulse is delayed 105 ns with respect to the electron pulse in our setup. Therefore, the ICCD setup does not allow collection of spectra at earlier time intervals.

Optional photodiode detectors are available in our PR setup (Table 2). The required wavelengths for the photodiodes are selected using 12.5-mm--diameter bandpass filters (Edmund Optics). They are changed using a homemade automatic filter wheel (controlled by an RS-485 interface). The FWHM is 10 nm for filters with a central wavelength <750 nm and 50 nm for those >750 nm. The cutoff filters are used together with the bandpass filters to eliminate undesirable transparent spectral ranges. Currently, three fast photodiodes are used in our system: (1) photodiode array PDA10A (Thorlabs) silicon-amplified photodiode, with a spectral range from 200 nm up to 1100 nm and a rise time of 2.3 ns; (2) a UV-enhanced, silicon APD430A2 (Thorlabs) avalanche photodiode, with a spectral range of 200–1000 nm and a rise time of 0.88 ns; this detector has continuously adjustable gain based on a diode multiplication factor control; (3) at the NIR spectral range (800–1700 nm), an InGaAs-amplified photodiode (PDA10CF; Thorlabs) with a rise time of 2.3 ns is used. Even though the spectral range of the PDA10A and APD430A2 photodiodes starts from 200 nm, more favorable noise-to-signal ratio is observed at wavelengths <520 nm for the PMT detector.

The electric output signals from the PMT and the photodiode detectors are digitized by WaveSurfer 104MXs-B (LeCroy) or HDO6104B (LeCroy) oscilloscopes. Vertical resolution of the WaveSurfer 104MXs-B is 8 bit, sampling rate is 10 GS/s, and bandpass is 1 GHz (limited to 200 MHz for typical experiments). The HDO6104B is a more powerful device, with 12-bit resolution, 1-GHz bandpass, and 10-GS/s sampling rate.

Recently, the development of a fast conductivity detection system based on Janata's [27] description is under implementation at the PR setup of the INCT.

Cell holders/flowing cell systems

The holders available in our setup are adapted to standard cells with 1 cm or shorter optical pathways. A longer optical pathway is not recommended due to the limited diameter of the cross section of the electron beam. In general, ~0.300 mL microcells or ~0.070 mL (dead volume) flow cells are used.

A special cell holder for temperature-dependence measurement is under development. This is a flow jacket construction with water-based heating factor. The temperature of the heating factor is controlled by CF41 cryo-compact circulator (Julabo). This is a fully automatic device communicating through an RS-485 interface. A T-type thermocouple, placed in the cell holder (in close vicinity of the cell), is used for accurate temperature measurements.

Two types of flow systems are available at the PR setup. The first is based on the Miniplus-3 peristaltic pump (Gilson). Its main function is automatic replacement of the irradiated solution with fresh one. Polymer (rubber, Teflon, polyether ether ketone [PEEK]) hoses used in the system are a source of limitation. This is due to the permeability of gases (e.g., O_2) through the polymeric material. The second flow system is based on two chromatographic P2.1S pumps (Knauer). This system is dedicated for concentration-dependence experiments. In addition, the stainless steel material used in this system is impenetrable for gases. Typically, both systems operate slightly below the flow rate of 1 ml·min^{-1}. Construction of a complete 3D spectrum requires ~100 ml of solution at this condition. Both flow systems are connected to the communication core of the PR setup and are fully computer-controlled.

Communication core

The PR system at the INCT is located in three remote rooms: the PR CR, the LAE-10 CR, and the irradiation chamber (PR IC). A layout of the facility is presented in Fig. 5. Physical connections between these localizations are necessary for transferring data, as well as for voice communication and visual monitoring. The two last functionalities are particularly important during system maintenance, equipment adjustment, repairing, and development.

The communication core was constructed based on Ethernet/Wi-Fi local area network (LAN) with transmission control protocol/Internet protocol (TCP/IP). This is the most reliable communication mechanism with respect to its cost. The possibility and simplicity of communication between large numbers of devices positively affect the flexibility of the PR system and open the way to a fast adaptation of the experimental environment on daily bases. This is particularly pronounced in combination with properly design software. Moreover, current common commercial applications of this type of communication guarantee that the Ethernet standard will be valid for at least the next 20 years. It certainly implies accessibility to various scientific instruments with compatible interfaces and the potential to be used as a part of the PR system.

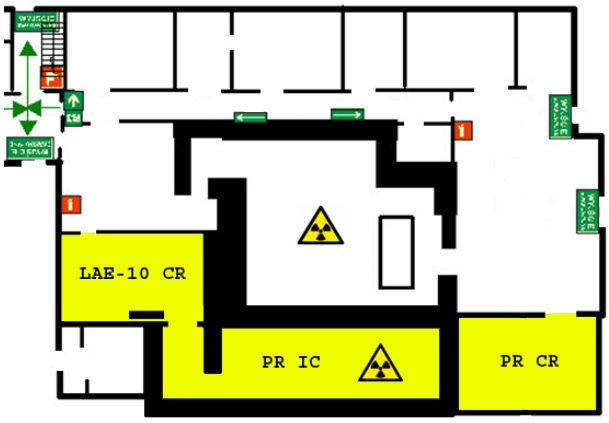

Fig. 5. Layout of the PR facility at the INCT.

All devices implemented into a system are addressed within private IP ranges starting from 192.168.0.0 with mask 255.255.0.0. Gate 192.168.0.1 is used rarely for temporary connection to wide area networks (WANs) in order to update software or device drivers.

The electromagnetic noise generated by the LAE-10 trigger system is transferred by the metal connectors and may affect the responses of detectors. Therefore, all PR facility rooms are connected only by multimode optical fibers (which do not transfer electromagnetic noises). An interroom fiber-optic network uses the 100Base-FX standard, whereas an intraroom communication system is based on a twisted-pair metal-connection network compatible with 10/100Base-TX standards. Local Wi-Fi (IEEE 802.11b/g/n) networks are used mainly for PR service and software development. The general scheme of the PR hardware connections is shown in Fig. 6.

ADAM 6000 Ethernet module series (Advantech) are preferably used in our system due to their versatility, damage resistance, and system protection capabilities (isolation protection up to 1000 V). The reliability of Advantech Corporation guarantees access to replacements of damaged components in the future. There are three different groups of ADAM modules implemented in the system: signal converters (Ethernet <–> fiber optics, Ehternet <–> RS-232/485), I/O analog or digital data modules, and relay modules. They are particularly useful in combination with homemade devices (e.g., shutter control, thermocouple readout). ICS Electronics's 9065 Ethernet-to-GPIB controllers are used for communication with GPIB devices and UE 204 Universal Serial Bus (USB) over IP Hub (B&B Electronics) for USB devices. There are some speed limitations of the latter converter. Therefore, the implemented devices must be carefully selected.

A new communication core was also crucial for replacing the old PR voice communication system between facility rooms. The previous system based on metal wire connections was a potential noise carrier. It was replaced by TCP/IP Ethernet phone communication. Moreover, Ethernet cameras were installed for visual monitoring of LAE-10 CR (particularly, control cabinet indicators) and PR IC (flow system monitoring).

It is important to note that construction of the new PR system was a time-consuming challenge. Shortening of the downtime of the instrument was a crucial issue from the economical point of view. Therefore, rebuilding of the system was formulated in a way that minimized interruptions in instrument operation. In fact, the previous system

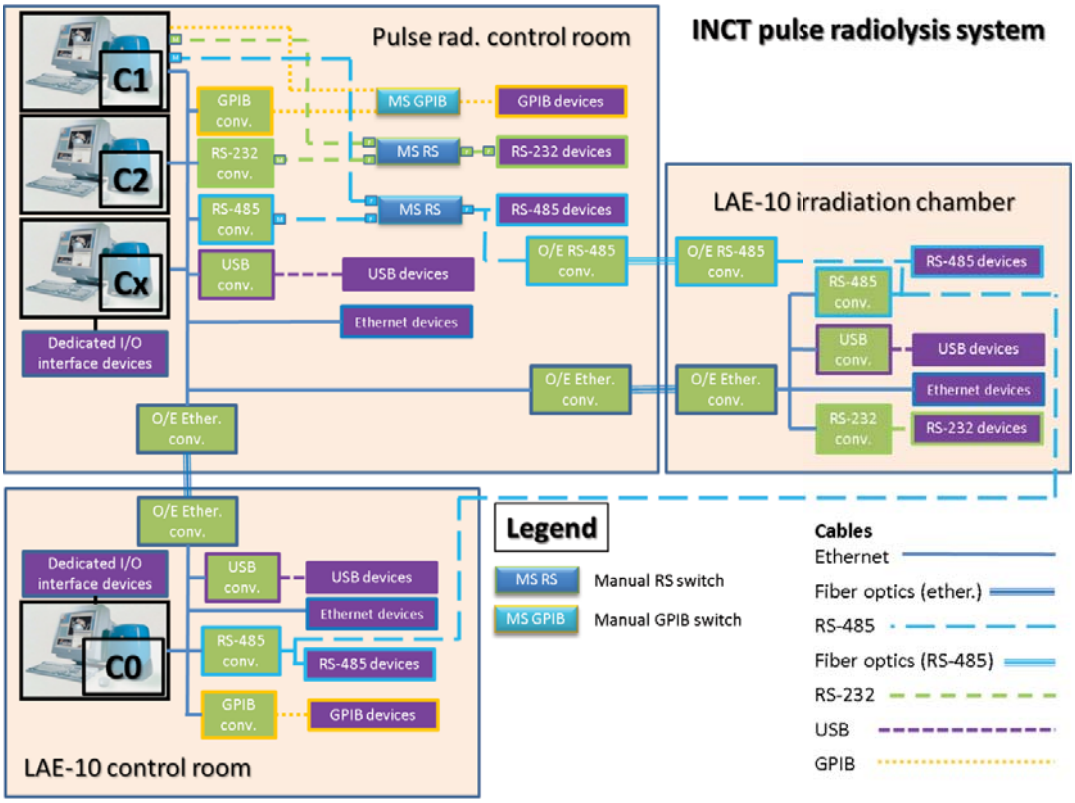

Fig. 6. Simplified scheme of the network/communication core at the INCT PR system.

was implemented into the new one. The computer controlling the previous system (C1 in Fig. 6), was implemented into the new system using several manual port switches (MS devices in Fig. 6), and the old communication core, based on RS-485, was included into the new system through an ADAM converter. This solution provided a "smooth" way for the changes to be made. Gradually, the old system was replaced by a new one, practically without any noticeable interruptions. In contrast to the previous system, data-collecting computers do not need to be equipped with any RS-232, RS-485, or GPIB cards. This simplifies the development of software. New versions of the programs can be developed on separate computers (connected just by Wi-Fi or twisted-pair cable) without any interruption in the working software version. Advanced, unique detection systems, such as an ICCD, may use a separate computer. This is due to the fact that an ICCD requires a dedicated computer I/O card. In this case, redundancy is the additional advantage of the new system since broken computer tasks can be easily overtaken by another computer attached to the system. Connected computers can easily exchange metadata through disk-sharing mechanism or Ethernet (SOCKET) protocol. This is crucial for the linkage of the LAE-10 accelerator and PR detection subsystems. Close interaction of these two systems is expected to improve the problem detection and diagnostic mechanism of LAE-10. Moreover, it shortens the time of the accelerator turn-on procedure on a daily basis and improves the accuracy of LAE-10 adjustment during experiment time. Currently, this solution is under development.

Laser flash photolysis (LFP) setup

Source of light pulse – Surelite II (Continuum) laser

The Nd:YAG Surelite II (Continuum) laser is a source of light pulse of the LFP setup at the INCT. The time duration of a light pulse is 6 ns (355 nm, FWHM) – measured as a quartz reflection by an avalanche diode photodetector. The basic line of the Surelite II is at 1064 nm. At this wavelength, the pulse energy is ~670 mJ. A built-in second harmonic generator produces a 532-nm line with energy in the pulse of ~310 mJ. From the application point of view, the most useful wavelengths of 355 nm and 266 nm are produced by the replaceable third and fourth harmonic generators. Energies in the pulses for both lines are ~100 mJ and 80 mJ, respectively.

Separation of a laser third or fourth line is performed by Surelite Separation Package (SSP, Continuum) based on a replaceable set of dichroic mirrors. Additional separation is achieved by perpendicular redirection of the laser beam toward the sample holder using high-energy mirrors: 10QM20M.45 (Newport) for the 355-nm line or 10QM20HM.75 (Newport) for the 266-nm line. The laser beam energy deposited on the surface of a typical quartz cell is higher than the damage threshold. Therefore, a plano-concave, fused-silica distracting lens with an effective focal length of –500 mm (SPC040AR.10, Newport) is used. Moreover, the timing of a Pockels cell of Surelite II is purposely misadjusted to work out of maximum power. A homemade shutter (described in the section "Source of electron pulse – the LAE-10 accelerator") is used for blocking

the laser pulse. This is necessary for recording the monitoring light trace.

The Surelite II provides a transistor–transistor logic (TTL) electric output signal for triggering the LFP detection system. There are two available sources of this signal: "fixed sync out" and "variable sync out". Both sources descend signals from the laser Pockels cell triggering pulse. "Variable sync out" provides a very useful time adjustment feature (from 325 ns before lasing), but its jitter with respect to the laser pulse is bigger than for "fixed sync out". "Fixed sync out" signal is delivered ~100 ns before lasing, with jitter of ~1 ns. Therefore, this source is typically used.

The energy of a laser pulse is monitored using two available setups: a 11MAESTRO (Standa) single-channel laser power energy mater; and a J25LP-MB (Coherent) sensor. For signal analysis, the J25LP-MB is connected to the 9304C (LeCroy) oscilloscope (8-bit analog-to-digital converter; sample rate 100 MS/s; bandwidth 200 MHz).

Detection system

A Hamamatsu Photonics K.K. setup is used as a monitoring light source. It consists of a quiet, low-noise L2273 (150 W) or, alternatively, ozone-free L2274 (150 W) xenon lamps. Lamps are placed in E7536 housing and powered by C7535 supply. This setup is similar to the one used in the PR system (Section "Source of electron pulse – the LAE-10 accelerator").

The optical pathway of the LFP monitoring light is relatively simple. It consists of three plano-convex F150 lenses (LB1374; focal length 150 mm, UV-fused silica; Thorlabs Inc.). Its simplified scheme is shown in Fig. 7.

Light exposition on sample is controlled by a mechanical shutter. This shutter is placed between a light source and the first F150 lens. The system is adapted to work with two types of shutters: a homemade shutter described in the section "Source of electron pulse – the LAE-10 accelerator"; and SH1/M (Thorlabs Inc.) shutter. The latter one is fully controlled by RS-232.

If it is required, the IR spectral range can be removed from the analyzing light by a water filter (10 cm). This filter is placed between a lamp and a shutter. In order to avoid reactions initiated by the monitoring light, UV or VIS cutoff filters are placed between the first lens and a sample holder. They are exchanged manually.

Wavelength selection is performed using a SpectraPro 275 (Acton Research) monochromator. This is an f/3.8, Czerny–Turner type of monochromator, with a focal length of 275 mm. The SpectraPro 275 uses three gratings. Their description is shown in Table 3. This device is fully controlled via an RS-232 interface.

The R955 (Hamamatsu) PMT is the most commonly used detector in our system. The PMT is attached to the SpectraPro 275 monochromator output port and placed in a homemade metal housing. The mechanical and electrical designs are much the same as in the PR system. Optionally, photodiode (PDA10A, APD430A2, and PDA10CF; all from Thorlabs) detectors are available at the LFP system. The technical specifications of all detectors are shown in Table 2, and a more detailed description is provided in the section "Source of electron pulse – the LAE-10 accelerator".

The electric signals from the PMT detector and the photodiodes are digitized by the WaveSurfer 104MXs-B (LeCroy) oscilloscope. Vertical resolution of the WaveSurfer 104MXs-B is 8 bit, sample rate is 10 GS/s, and bandpass is 1 GHz (limited to 200 MHz for a typical experiment).

Cell holders/flowing cell systems

The LFP system is equipped with a standalone Flash 300 (Quantum North West) cell holder. Its isolated, temperature-controlled housing is adapted to standard 1-cm-optical path cells. The position of the holder with respect to the light beams is adjusted by built-in micrometers. The temperature of Flash-300 is set using a TC 125 temperature controller using Peltier thermoelectric modules. The operating temperatures of Flash-300 range from –55°C to 105°C (±0.02°C).

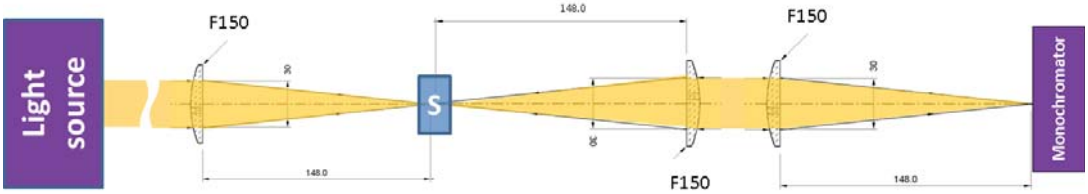

Fig. 7. Optical pathway of the monitoring light of the LFP system. S – sample; F150 – lenses.

Table 3. Description of SpectraPro 275 monochromator gratings

ID	Range of application (nm)	Blaze (nm)	Lines (g/mm)	Resolution per slit size (nm/mm)	Comment
1	200–310	250	1800	30	–
2	310–570	500	1200	10	BK-7 cutoff filter (or its equivalent) should be used at wavelengths >415 nm
3	550–1200	1000	600	20	RG-5 filter (or its equivalent) should be used at wavelengths >685 nm

For low-temperature ranges, a special windowed jacket preventing condensation on the cell is used.

Commonly, a gravitation flow system is used at the LFP. However, there is a possibility of using systems based on a syringe pump (KDS-270-CE; KD Scientific) or peristaltic Miniplus-3 pump (Gilson) if it is required.

Both the Flash-300 and the flow cell systems can be controlled by a computer. However, this is an unnecessary complication since all instruments are within the operator's reach.

Communication core

The communication core of the LFP setup is constructed based on the Ethernet/Wi-Fi LAN with TCP/IP. Since the entire LFP technique is localized in one laboratory room, the communication core is much simpler than the PR local network. All devices are addressed within a private IP range starting from 192.168.0.0 with mask 255.255.0.0. In general, the addresses of the devices are identical to their equivalent in the PR system. Gate 192.168.0.1 is used rarely for temporary connection to WAN in order to update software or device drivers. Local Wi-Fi (IEEE 802.11b/g/n) network is used only for LFP service or software modification.

Software

The construction of new software is guided by several key principles. They were established on the basis of the experience gained by the author operating several time-resolved, pulsed-technique facilities at various scientific institutions. The open architecture of the software is one of the most important issues. The designed block-based software system structure is, inter alia, an implementation of this principle. It turns the designed system to a relatively expandable, improvable, and flexible experimental environment. This is particularly valid if the designed software is combined with the flexibility of communication cores such as Ethernet. Independent blocks/programs are responsible individually for controlling/monitoring of one particular device or a group of devices performing a common particular subtask. This solution has many advantages over a single application controlling an entire system. Both LFP and PR systems can share the same blocks/programs depending on the current system setups. Each block/program can be tested and developed separately outside of the entire system. Daily-based, hardware system adaptation to experimental requirements is reflected in running corresponding blocks/programs. It eliminates the effect of consumption of computer resources by software handling the drives of unused devices and keeps software dependency as simple as possible. In addition, block/program solution is characterized by high redundancy. Malfunctioned computer-controlled devices, with no critical meaning for the current experiment (e.g., a filter wheel that can be positioned manually), can be disconnected from the system by closing the corresponding application. This kind of problems may cause difficulties, but they are not expected to stop an entire experiment. The other advantage is due to the fact that each block/program runs its code independently. Therefore, several instruments may simultaneously be monitored/may perform their tasks. In some situations, this significantly shortens the time of the experiment. However, a similar effect can be achieved with a single application by using multithreading, but this unnecessarily complicates coding and makes the debugging process relatively complex. Short and simple code is a very important criterion for "smooth" debugging, fast compilation, and simplicity of future improvement/development process. It is worth mentioning that for such a system, each of the next blocks/programs can be coded in any environment depending on the developer's preferences. Knowledge or understanding of previously written codes is not required. The block/program communication method and the command syntax constitute sufficient information for integration of a new segment with the system.

Full automation of data collection is another important key principle of the new system. It shortens the experimental time and eliminates some possible human errors occurring during long and repetitive collection procedures. The greatest benefits of measuring automation are for data collections related to 3D spectra or temperature dependencies. Automation requires the reliability of the operating system (OS) and the applications running under it. Thus, it is important that the OS is not too heavy and the designed applications are expected to be light and bug-free. Light block/program (a requirement mentioned earlier) is one of the most important factors significantly improving the clearance of a code. It results in elimination of unpredicted exceptions and thus improving the reliability of a single application and the whole system.

The general programming tendency is to create human-error-resistant applications. In major cases, this is the most difficult and time-consuming stage of programming. The possibility of elimination of all undesired user behaviors thus decreases significantly with the complexity of the application. Therefore, there is a valid reason to keep all applications simple. On the other hand, an extensive human-error-protected application may limit the capability of computer-controlled instrumental systems. Therefore, the clue is to find a balance between human error protection and easy/fast access to all instrument capabilities. According to author experience, in all LFP and PR facilities, only selected, skilled personnel have full access to sophisticated instruments. This is particularly valid for homemade systems. Skilled instrument operators are not expected to take random "clicking" actions; however, they can make an accidental error. Therefore, protection of expensive hardware, particularly from irreversible damage, is a priority and should be taken with maximum extension. However, other operators' actions should be considered as intentional. Warning is expected to accompany selected, unusual actions, but program

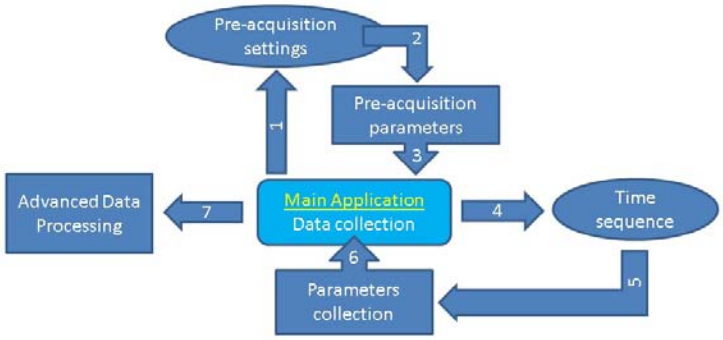

Fig. 8. Simplified block diagram of the TSFF system communication.

stopping with error message should be rarely used – only for critical issues. Transparent and extensive history of all operations and events is required for this system.

An application package meeting the assumptions described above was designed, coded, and named TSFF. Currently, version 4.0 is implemented at the PR and LFP at the INCT. The system is built of several applications/blocks. Their dependencies are shown in the simplified block diagram presented in Fig. 8.

The Main Application is the center of the TSFF software system. General attention of the PR operator is focused on this application. Collection of data is initiated by pressing a button related to the desired experimental mode of action. At first, the measurement parameters of the main data collection device (e.g., oscilloscope) are set. After that, the Main Application transfers the preacquisition settings to the blocks/programs responsible for controlling related, external devices, and then it waits until all the required preacquisition parameters (e.g., wavelength, temperature) are transferred back. Subsequently, a time sequence is initiated. During this stage, a high-energy pulse is delivered to the sample, and the postpulse parameters (e.g., pulse energy) are collected. After the time sequence finishes its tasks, the Main Application downloads the collected experimental data from the main data collection device. It also roughly performs evaluation of the collected information. The compliance of parameters with the imposed limits and the physical correctness of the data are verified. Then, the data are preprocessed and transferred to the advanced data processing application.

The *Digitizer* (ver. 2.0), *DeviceCtrl* (ver. 4.0), *Sqnc* (ver. 3.0), and *Mnhr* (ver. 2.0) are the basic applications that control data collections in the TSFF package. All are designed under the Delphi XE2 (Embarcadero) development environment.

The *Digitizer* plays the role of the Main Application. It controls the oscilloscope's I/O operations and controls the transfer of data between TSFF blocks/programs. The main tab of the graphical user interface (GUI) of the *Digitizer* is shown in Fig. 9.

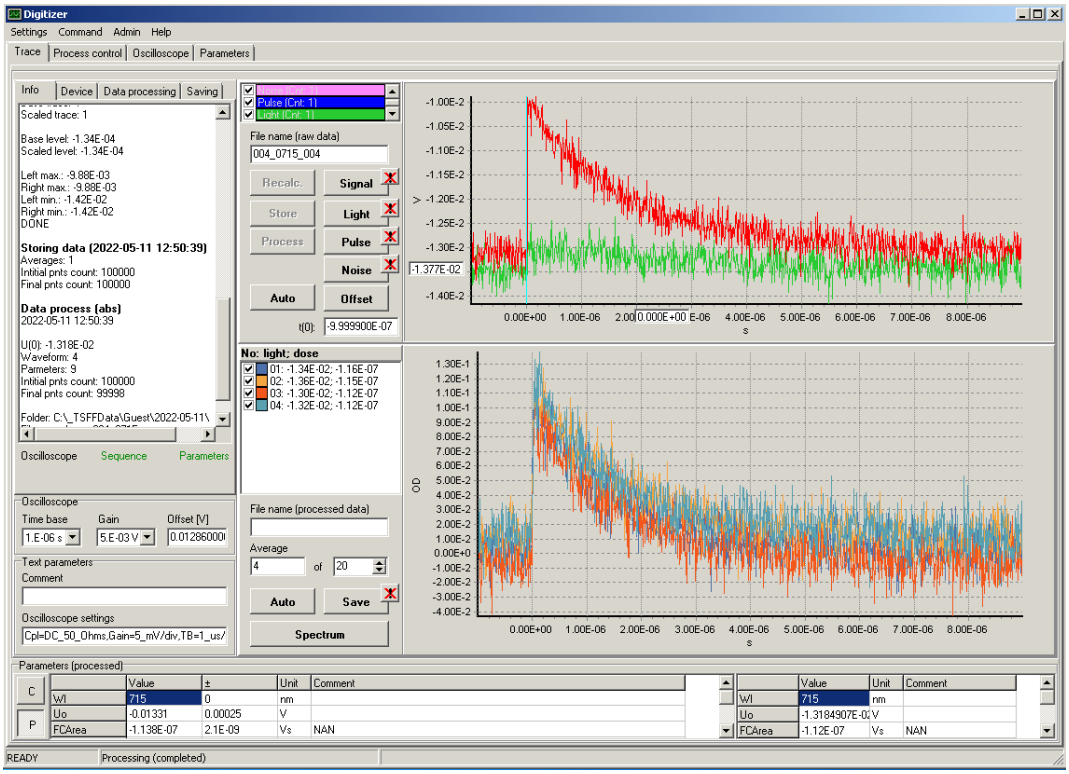

Fig. 9. Graphical user interface of the *Digitizer* application.

Table 4. Description of types of data time traces collected by *Digitizer* application

Type of trace	Incident beam	Monitoring light shutter	Description
SGN(t)	ON	ON	This trace carries the main information about the chemical/physical changes of the irradiated sample.
LIGHT(t)	OFF	ON	Trace carries information about the shape of the monitoring light. It is optionally used to correct the resulting output for time-dependent monitoring of light fluctuations.
PULSE(t)	ON	OFF	Response of the detection system on the incident beam pulse. Important for elimination of emission of sample from absorption output data.
NOISE(t)	OFF	OFF	Response of detection system on electromagnetic noise generated due to triggering of high-energy incident pulse. In general, it is used for diagnostic purpose or automatic measurement of optical detector offset current. In some cases, it can be used to eliminate electromagnetic, reproducible noise from the detector output (if it is not possible to eliminate noise by hardware handling).

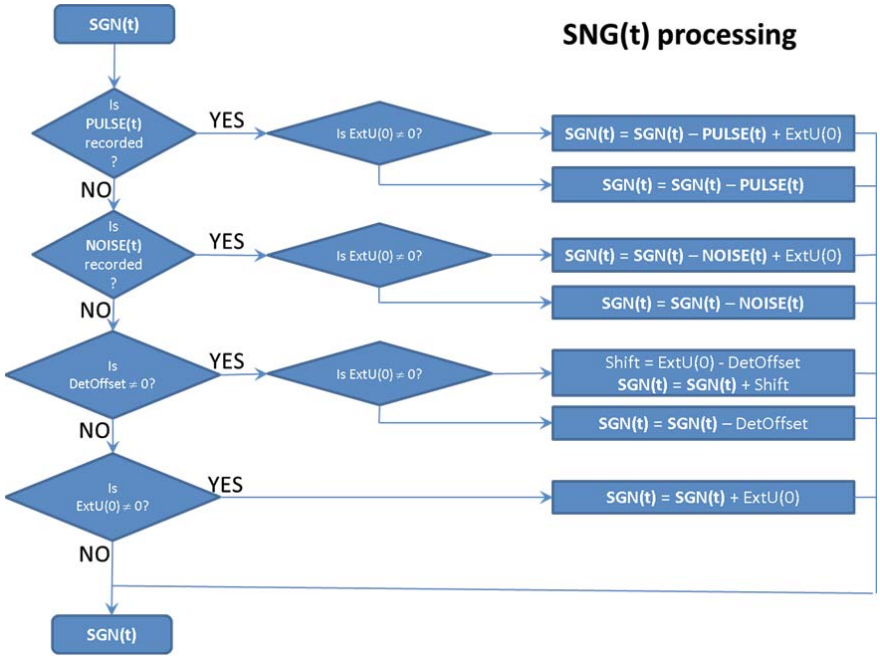

Fig. 10. Algorithm of SGN(t) trace preprocessing. DetOffset is the detector offset value; ExtU(0) denotes the absolute value of the light level measured by the external device (so-called back-off system).

The current version of the *Digitizer* application is capable of working with LeCroy oscilloscopes. Communication is established through DSO ActiveX control. Depending on the needs, other types of oscilloscopes can be implemented (e.g., Tektronix). The *Digitizer* application handles both emission and absorption measurements. Mechanisms for collection of the four types of data/time traces (SGN(t), LIGHT(t), PULSE(t), and NOISE(t)) are implemented in the *Digitizer*. Time trace types are described in Table 4. Collection of LIGHT(t), PULSE(t), and NOISE(t) signals is optional and depends on the experimental requirements.

The data downloaded from an oscilloscope are preprocessed by the *Digitized* application at the beginning according to the algorithm diagram presented in Fig. 10. The main idea of preprocessing is to remove/clean SGN(t) from all undesired signals. In addition, correction of SGN(t) for detector offset (DetOfffset, Fig. 10) is carried out. This is necessary for most of the diode detectors, which are characterized by nonzero responses in the dark (without incident light). Optionally, the *Digitizer* application allows to use an absolute level of light value (ExtU(0), Fig. 10) measured by an external device (often called the back-off system); otherwise, the light level is calculated based on the cleared, selected range of SGN(t) traces.

In the case of time-dependent light level, it is necessary to collect LIGHT(t) trace for SGN(t) data correction. Preprocessing of a LIGHT(t) trace is shown in Fig. 11.

Finally, the transient optical absorption (PROC(t)) of the system is calculated based on the algorithm diagram shown in Fig. 12. Note that SGN(t) trace was already corrected by an optional, absolute level of light (ExtU(0)) as well as the detector offset value (DetOffset, Fig. 10). Thus, the obtained U(0) value corresponds to a real light level. In particular cases, it is necessary to make

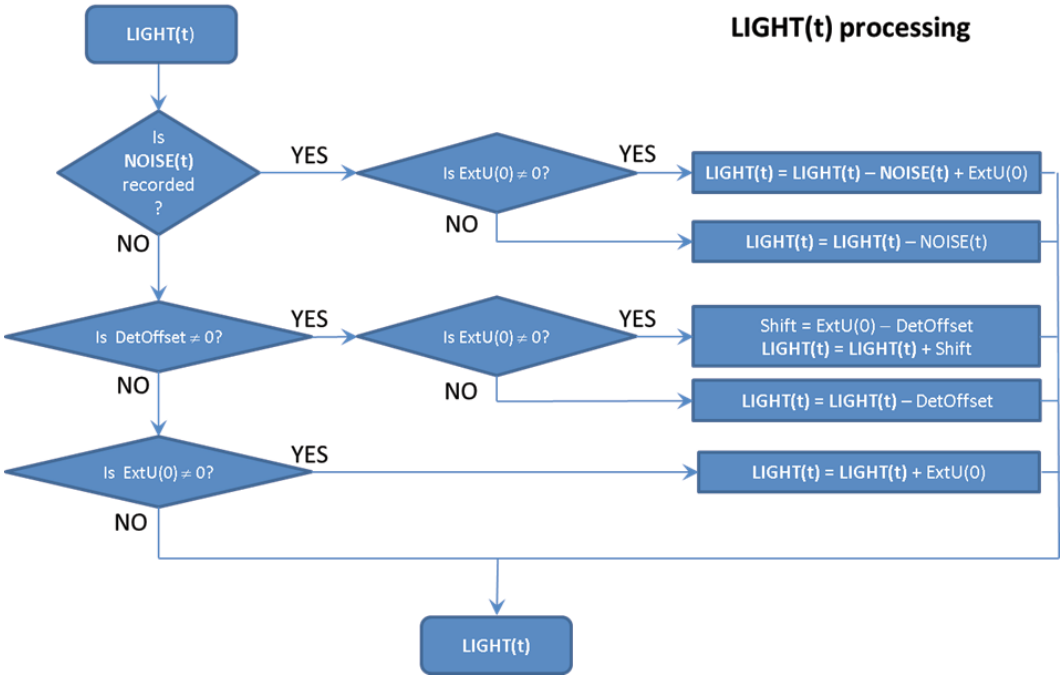

Fig. 11. Algorithm diagram of LIGHT(t) trace processing.

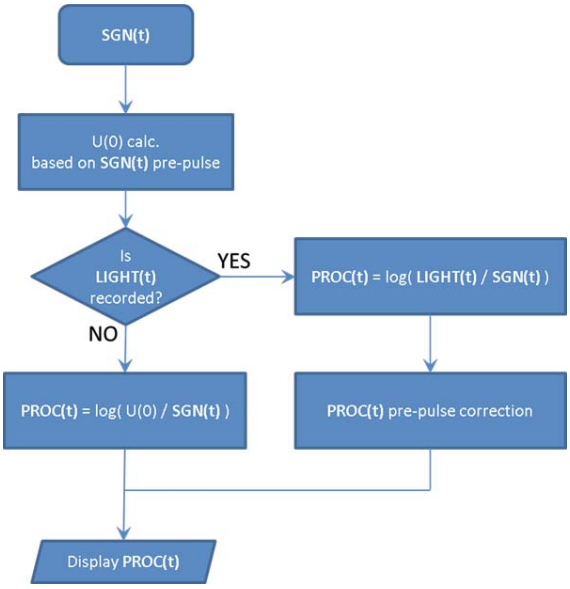

Fig. 12. Algorithm diagram for calculation of optical absorption of the investigated system based on traces recorded by the oscilloscope. U(0) is the light level calculated based on the selected range of SGN(t) prepulse trace.

an additional correction of the PROC(t) trace by a nonzero prepulse value. This is when a slow fluctuation in the amplification factor of monitoring light occurs. It is observed in the case of monitoring light pulsing. Changing of the vertical position of the LIGHT(t) trace on the oscilloscope with remaining shape stability is the most pronounced symptom of this situation.

It is possible to run more than one instance of the *Digitizer* application in the TSFF system. In this case, additional *Digitizer* applications play a "slave" role. They allow collection of the data from more than one detection systems using spare oscilloscope channels or even additional oscilloscopes.

The *DeviceCtrl* application is mainly used to set/read the preacquisition parameters (e.g., pump flow rates, temperature of circulator, and polarization voltage of electron gun grid) to/from external instruments (Fig. 8). Information required for coupling of the *DeviceCtrl* application with an external device is located in the configuration file. The file contains settings of the communication interface, control commands, and application options. Therefore, different external devices are handled by different instances of this application. The *DeviceCtrl* application works with any instrument supporting standard communication protocols (serial communication, GPIB, and TCP). This application dynamically links National Instrument Corporation, Virtual Instrument Software Architecture (NI-VISA) library. Currently, version 17.5 of NI-VISA is used by the TSFF system. Alternatively, the *DeviceCtrl* application is capable of communicating with external devices through author-designed or standard Delphi components (such as Indy components). In some cases, these alternative approaches give better control results. There are two available GUIs of the *DeviceCtrl* application, i.e., the commonly used simplified GUI and the advanced one. Both are shown in Fig. 13. The *DeviceCtrl* application has several useful features, such as (i) selection of a parameter value from a

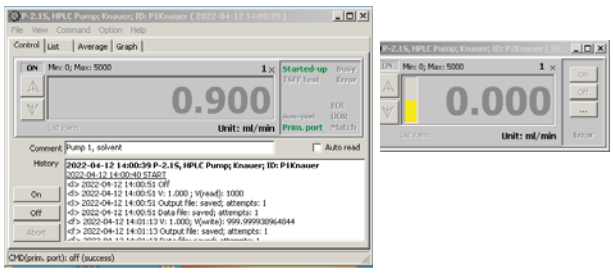

Fig. 13. Examples of advanced (left) and simplified (right) user interfaces of the *DeviceCtrl* application.

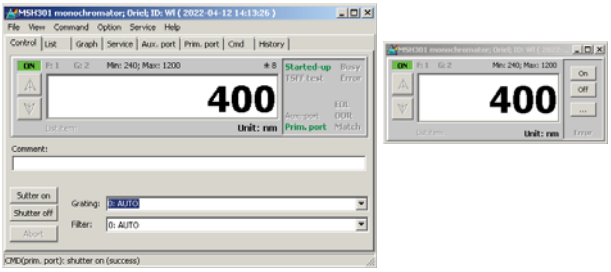

Fig. 14. Advanced (left) and simplified (right) graphical user interface of *Mnhr* application.

preprepared list, (ii) capability of returning the average parameter value instead of a single measured value, (iii) graphical presentation of both sets, and (iv) reading values as a function of time.

The *Mnhr* is a monochromator-managing application. It is descendent of the *DeviceCtrl* application. Both applications share common features. The differences are connected with the specific functions for the monochromator. Therefore, mechanisms for handling of grating, cutoff filter changer, and built-in shutter are implemented in *Mnhr*. The GUI of the *Mnhr* application is shown in Fig. 14.

The *Sqnc* is an application that runs a sequence of operations on external devices leading directly to experimental data collection (arming accelerator, shutter open/close operation, electron pulse triggering, energy of pulse collection etc.). Devices controlled by the *Sqnc* application and the time-sequence operations are declared in the configuration file. Thus, modification of the instrumental sequence is limited to modification of the configuration file. There is no need to interfere in the program code. An example of a *Sqnc* GUI is shown in Fig. 15. The *Sqnc* and *DeviceCtrl* applications share the same system of communication with external devices.

Depending on the experimental setup, there are some other applications dedicated to specific instruments. For instance, the Surelite II (Continuum) laser is managed by the SL2 application in the LFP. The SL2 application is responsible for warming/cooling, adjustment, and reporting stability of the laser.

Currently, all blocks/programs of the TSFF system use text or binary files for exchanging metadata and passing control commands. All commands

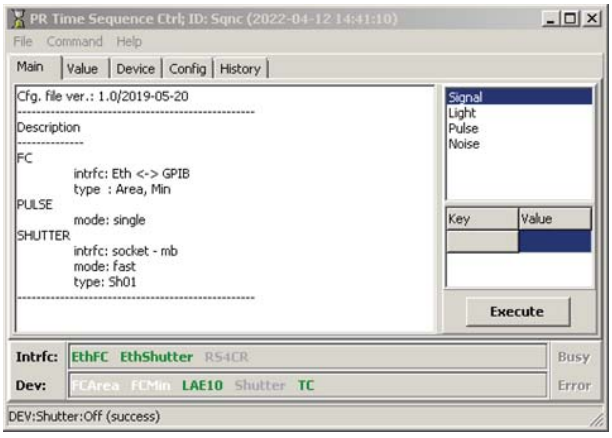

Fig. 15. User interface of the *Sqnc* application.

for particular blocks/programs are addressed by unique IDs. Commands with not-matching IDs are passed from the input to the output stream of blocks/programs, allowing sequential performance of some operations. Ethernet/SOCKET-based communication is currently under implementation. In both cases, efficient and reliable communication between blocks/programs is established even for applications running on remote computers. The code of each designed application is relatively short and does not exceed 8000 lines in the main file. All applications work in both user and administrator modes. Administrator mode is password protected since interference in administrator functions may cause instability of the system or even external device damage. Each application of the TSFF system has a clear encountered problem-reporting mechanism. Problems are announced by voice as well as visual messages. All applications have implemented the mechanism of automatic problem solving. They are capable of recovering without disruption of the experiment, even in the case of physical disconnection of the cable between the computer and the external device – as long as reconnection is done within the time-out value. All state changes (including exceptions) of blocks/programs are saved in the log files. They help to maintain the system and solve possible problems.

For user convenience, starting up of the entire TSFF system is done by batch script code, which can be easily profiled according to particular user preferences. In addition, batch scripts are expected to make general maintenance of the entire TSFF system (cleaning temporary files, creating experimental folders, as well as data and system backups) easy. They are executed from the user interface shown in Fig. 16.

Short codes in Python 3.8 play a role of batch script enhancement. For instance, such a code is used to obtain a required concentration of a solution using a P2.1S pump (Knauer) flow system. Pumps are directly controlled by the *DeviceCtrl* applications. However, from the user point of view, it is inconvenient to manually calculate the flow on each pump to receive the required concentration. Thus, pumps flows are calculated based on the concentration value processed by the Python codes.

The last important part of the TSFF system is the advanced data processing application (Fig. 17). It was designed under Igor Pro 7 (WaveMatrix) environment. The Igor Pro is an integrated application for visualizing, analyzing, transforming, and presenting experimental data. It is capable of handling large data sets (including waveforms) with a relatively high speed. There is the possibility of automation and data processing in the programming environment. Codes written in Igor Pro 7 are precompiled at the start of the application. This results in relatively fast subsequent data processing. The programming feature was used to perform automatic processing of data collected by time-resolved techniques. The designed and written code was encapsulated in a "macro" named TSUC. Numerous functions for transformation of vertical and horizontal scales, building 2D and 3D spectra, fitting experimental

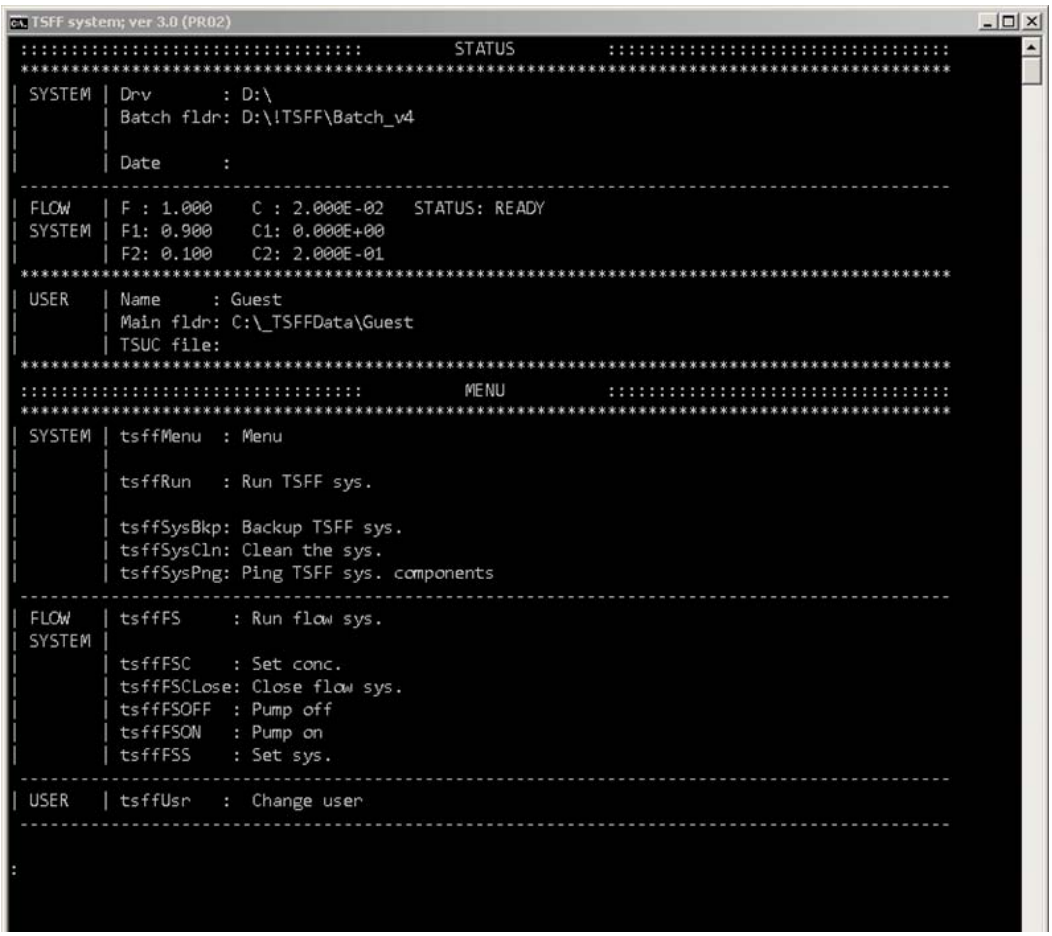

Fig. 16. TSFF package batch script execution interface.

data to kinetic models, etc., are implemented. The TSUC processes data passed by the *Digitizer* application on the fly – data can be loaded during an experiment or after the experiment is done. In fact, the implemented TSUC mechanisms allow the loading and processing of experimental data from all time-resolved techniques at the INCT (namely, PR, LFP, and stopped-flow techniques) and also from

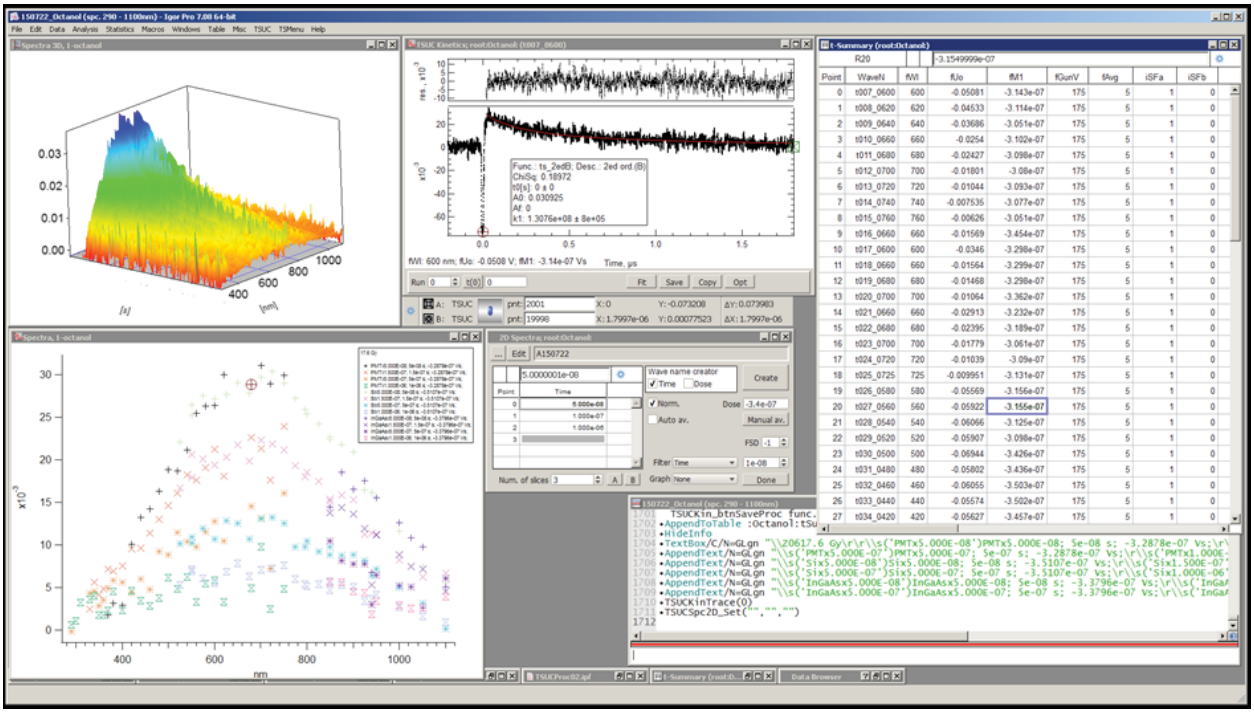

Fig. 17. The advanced data processing application (TSUC).

instruments at collaborating laboratories, such as the Institute of Applied Radiation Chemistry in Lodz (Poland), ELYSE Université Paris-Saclay in Paris (France), Universidad de Chile in Santiago (Chile), or the Laser Electron Accelerator Facility at Brookhaven National Laboratory at Long Island (NY, USA).

The TSFF application significantly shortens the time of data collection in comparison to the previous system. In general, the monitoring light shutter is opened for ~1 s. A short open/close cycle is important for light-sensitive samples, particularly when a 1-kW xenon lamp is used. Currently, it takes ~25 min to collect the UV–VIS spectrum, with three averages for each time profile using a regular single-mode technique. This can be even faster using the so-called multipulse mode. In this mode, the monitoring light shutter is opened, several electron/light pulses (number depends on the settings) are delivered to the sample, and then, the shutter is closed. Maximum pulse repetition is ~3 Hz in both PR and LFP setups. It is limited by the capabilities of the oscilloscopes to collect the data and rearm. Data averaging is performed by the oscilloscope software without transferring to the controlling computer between pulses. This mode does not allow investigation of all types of samples since a high pulse repetition makes it impossible to remove the products of the reaction by the flow system.

Conclusions

Upgrading of the PR detection system and construction of a new LFP system were carried out at the INCT in Warsaw (Poland). Implementation of a new powerful light source, extended collection of detectors, and optimization of the optical light resulted in the broadening of the experimental spectral range of the PR technique. The currently available spectral range is between 250 nm and 1700 nm. The modifications also caused noticeable reduction in the noise-to-signal ratio with respect to the previous setup. Improvement of the data quality and shortening of the data collection time were achieved by the new flow cell systems based on chromatographic pumps. The LFP system was built from scratch. Both LFP and PR systems were designed intentionally to share the same hardware and software solutions. Therefore, the components can be easily exchanged between the two systems, which significantly lowered the costs and shortened construction time. Opened architecture and improved experimental flexibility of both techniques were achieved by implementation of communication cores based on the Ethernet TCP/IP and newly designed computer-controlling software. This is the most important upgrade allowing the "smooth" and fast expansion of both setups in the future. Implementation of new components into these systems hardly ever requires programming. Moreover, daily adaptation of the hardware to the experimental requirements is significantly easier with respect to the previous setup. In addition, new, available experimental modes significantly reduced the collection time and improved the quality of the resulting data.

Acknowledgments. The author wishes to thank Prof. K. Bobrowski for helping in paper preparation and fruitful discussions, Dr. K. Skotnicki for helping in PR system maintenance, Dr. R. Kocia and Dr. P. Wiśniowski for solving administration issues, as well as S. Bułka and D. Pujdak for maintenance of the LAE-10 accelerator.

ORCID

T. Szreder http://orcid.org/0000-0003-0074-6315

References

1. Norrish, R. G. W., & Porter, G. (1949). Chemical reactions produced by very high light intensities. *Nature, 164*(4172), 658–658. DOI: 10.1038/164658a0.
2. Porter, G. (1950). Flash photolysis and spectroscopy a new method for the study of free radical reactions. *Proc. R. Soc. London Ser. A-Math. Phys. Eng. Sci., 200*(1061), 284–300. DOI: 10.1098/rspa.1950.0018.
3. Hague, D. N. (1969). Experimental methods for the study of fast reactions. In C. H. Bamford & C. F. H. Tipper (Eds.), *Comprehensive chemical kinetics* (Vol. 1, pp. 112–179). Elsevier.
4. Hart, E. J., & Boag, J. W. (1962). Absorption spectrum of hydrated electron in water and in aqueous solutions. *J. Am. Chem. Soc., 84*(21), 4090–4095. DOI: 10.1021/Ja00880a025.
5. Boag, J. W., & Hart, E. J. (1963). Absorption spectra in irradiated water and some solutions – absorption spectra of hydrated electron. *Nature, 197*(486), 45–47. DOI: 10.1038/197045a0.
6. Matheson, M. S., & Dorfman, L. M. (1960). Detection of short-lived transients in radiation chemistry. *J. Chem. Phys., 32*(6), 1870–1871. DOI: 10.1063/1.1731035.
7. Keene, J. P. (1960). Kinetics of radiation-induced chemical reactions. *Nature, 188*(4753), 843–844. DOI: 10.1038/188843b0.
8. Mccarthy, R. L., & Maclachlan, A. (1960). Transient benzyl radical reactions produced by high-energy radiation. *Trans. Faraday Soc., 56*(8), 1187–1200. DOI: 10.1039/Tf9605601187.
9. Novak, J. R., & Windsor, M. W. (1968). Laser photolysis and spectroscopy – a new technique for study of rapid reactions in nanosecond time range. *Proc. R. Soc. London Ser. A-Math. Phys. Eng. Sci., 308*(1492), 95–110. DOI: 10.1098/rspa.1968.0210.
10. Scaiano, J. C. (1983). Early history of laser flash-photolysis. *Accounts Chem. Res., 16*(7), 234. DOI: 10.1021/Ar00091a601.
11. Hentschel, M., Kienberger, R., Spielmann, C., Reider, G. A., Milosevic, N., Brabec, T., Corkum, P., Heinzmann, U., Drescher, M., & Krausz, F. (2001). Attosecond metrology. *Nature, 414*(6863), 509–513. DOI: 10.1038/35107000.
12. Wishart, J. F., & Nocera, D. G. (1998). *Photochemistry and radiation chemistry, complementary methods*

for the study of electron transfer. Washington, DC: American Chemical Society.
13. Bobrowski, K. (2005). Free radicals in chemistry, biology and medicine: contribution of radiation chemistry. *Nukleonika*, *50*(Suppl. 3), S67–S76.
14. Karolczak, S. (1999). Pulse radiolysis – experimental features. In J. Mayer (Ed.), *Properties and reactions of radiation induced transients* (pp. 11–37). Warszawa: Polish Scientific Publishers PWN.
15. Belloni, J., Crowell, R. A., Katsumura, Y., Lin, M., Marignier, J. -L., Mostafavi, M., Muroya, Y., Saeki, A., Tagawa, S., Yoshida, Y., De Waele, V., & Wishart, J. F. (2010). Ultrafast pulse radiolysis methods. In J. F. Wishart & B. S. M. Rao (Eds.), *Recent trends in radiation chemistry* (pp. 121–160). World Scientific.
16. Baxendale, J. H., & Busi, F. (1982). *The study of fast processes and transient species by electron pulse radiolysis*. (Nato Science Series C: Mathematical and Physical Sciences, Vol. 86). Dordrecht: Springer.
17. Kadlubowski, S., Sawicki, P., Sowinski, S., Rokita, B., Bures, K. D., Rosiak, J. M., & Ulanski, P. (2018). Novel system for pulse radiolysis with multi-angle light scattering detection (PR-MALLS) – concept, construction and first tests. *Radiat. Phys. Chem., 142*, 9–13. https://doi.org/10.1016/j.radphyschem.2017.04.010.
18. Zimek, Z. (1990). A new electron linac for puls radiolysis experiments at the Institute of Nuclear Chemistry and Technology, Poland. *Radiat. Phys. Chem., 36*(2), 81–83.
19. Mirkowski, J., Wiśniowski, P., & Bobrowski, K. (2001). A nanosecond pulse radiolysis system dedicated to the new LAE 10 accelerator in the INCT. In *Annual Report 2000* (pp. 31–33). Warsaw: Institute of Nuclear Chemistry and Technology.
20. Szreder, T., Schmidt, H., & Modolo, G. (2019). Fast radiation-induced reactions in organic phase of SANEX system containing $CyMe_4$-BTPhen extracting agent. *Radiat. Phys. Chem., 164*, 108356. DOI: 10.1016/j.radphyschem.2019.108356.
21. Marchini, M., Baroncini, M., Bergamini, G., Ceroni, P., D'Angelantonio, M., Franchi, P., Lucarini, M., Negri, F., Szreder, T., & Venturi, M. (2017). Hierarchical growth of supramolecular structures driven by pimerization of tetrahedrally arranged bipyridinium units. *Chem.-Eur. J., 23*(26), 6380–6390. DOI: 10.1002/chem.201700137.
22. Kocia, R. (2019). Pulse radiolysis studies of intermediates derived from p-terphenyl in the oxygenated methyltributylammonium bis[(trifluoromethyl)sulfonyl]imide ionic liquid. *Int. J. Chem. Kinet., 51*(12), 958–964. DOI: 10.1002/kin.21323.
23. Szreder, T., Kisala, J., Bojanowska-Czajka, A., Kasperkowiak, M., Pogocki, D., Bobrowski, K., & Trojanowicz, M. (2022). High energy radiation – induced cooperative reductive/oxidative mechanism of perfluorooctanoate anion (PFOA) decomposition in aqueous solution. *Chemosphere, 295*, 133920. DOI: 10.1016/j.chemosphere.2022.133920.
24. Zimek, Z. (2019). The INCT electron accelerator research facilities. In A. G. Chmielewski & Z. Zimek (Eds.), *Electron accelerators for research, industry and environment – the INCT perspective* (pp. 7–30). Warsaw: Oficyna Wydawnicza Politechniki Warszawskiej.
25. Beck, G. (1976). Operation of a 1P28 photomultiplier with subnanosecond response time. *Rev. Sci. Instrum., 47*(5), 537–541. DOI: 10.1063/1.1134685.
26. Chatgilialoglu, C., Krokidis, M. G., Masi, A., Barata-Vallejo, S., Ferreri, C., Terzidis, M. A., Szreder, T., & Bobrowski, K. (2019). New insights into the reaction paths of hydroxyl radicals with purine moieties in DNA and double-stranded oligodeoxynucleotides. *Molecules, 24*(21), 3860. DOI: 10.3390/molecules24213860.
27. Janata, E. (1982). Pulse-radiolysis conductivity measurements in aqueous-solutions with nanosecond time resolution. *Radiat. Phys. Chem., 19*(1), 17–21. DOI: 10.1016/0146-5724(82)90043-7.